

Effects of Longitudinal Photons

Christer Friberg* and Torbjörn Sjöstrand*

*Department of Theoretical Physics,
Lund University, Lund, Sweden*

Abstract

The description of longitudinal photons is far from trivial, and their phenomenological importance is largely unknown. While the cross section for direct interactions is calculable, an even more important contribution could come from resolved states. In the development of our model for the interactions of (real and) virtual photons, we have modeled resolved longitudinal effects by simple multiplicative factors on the resolved transverse-photon contributions. Recently, a first set of parton distributions for longitudinal virtual photons has been presented by Chýla. We therefore compare their impact on some representative distributions, relative to the simpler approaches.

*christer@thep.lu.se, torbjorn@thep.lu.se

1 Introduction

The interactions of a real photon are nontrivial, since the photon can fluctuate into partly non-perturbative $q\bar{q}$ hadron-like states. These strongly-interacting states actually are responsible for the bulk of the γp and $\gamma\gamma$ cross sections. In the spirit of hadronic physics, it is necessary to introduce parton distribution functions (PDF's) in order to describe jet production, with non-perturbative boundary conditions at some low μ_0^2 scale followed by a perturbatively defined evolution towards larger μ^2 . Also like in hadronic physics, a description of total, elastic and diffractive cross sections tends to rely on Regge type phenomenology, but again with many unknowns. The hadron-like interaction types are complemented by the direct interactions of the photons, to form a photoproduction framework.

In moving from the real to the virtual photon, matters do not become any simpler. Granted, once the photon virtuality Q^2 is very large, the deeply inelastic scattering (DIS) language of ep collisions can be used quite successfully, but this language bears little resemblance with the one used for real photons, and cannot be extended to small Q^2 . So, in the intermediate region, say $Q^2 \sim m_\rho^2$, physics is at best a bit of each, at worst beyond either of the two frameworks. In a set of two recent articles [1, 2] we have tried to develop a model that should provide a smooth interpolation between the photoproduction and the DIS regions, in the first article studying jet production and in the second the total cross section of events.

A special problem here is the contribution from longitudinal photons. By gauge invariance we know that longitudinal photon interactions must vanish in the limit $Q^2 \rightarrow 0$. However, in the few instances where their effects have been measured at nonvanishing Q^2 , the contribution has been quite significant, from vector meson polarization in exclusive reactions [3] to the standard DIS analysis of $R = \sigma_L^{\gamma^*p} / \sigma_T^{\gamma^*p}$ at small x and Q^2 [4]. Furthermore, in QED processes like $e^+e^- \rightarrow e^+e^-e^+e^-$ the longitudinal contributions are non-negligible [5, 6, 7]. Some of these contributions can be given a partonic interpretation, so it would be tempting again to use the time-honoured parton-distribution language. This is not a universally accepted route, but we may recall the successes in describing much of the diffractive phenomenology in terms of a partonic structure of the Pomeron [8], a state about as virtual and elusive as the longitudinal photon.

Recently a first set of PDF's for the longitudinal photon was presented by Chýla [5]. While the analysis is sensitive to the non-perturbative input for predictions at small Q^2 , this sensitivity is reduced for larger Q^2 . Access to sensible PDF's should allow an improved predictivity for a number of observables, compared with our previous approach of using simple Q^2 - and μ^2 -dependent factors to estimate the potential impact of the longitudinal-photon contribution. It is noteworthy that the total γ^*p and $\gamma^*\gamma^*$ cross sections do contain low- p_\perp components as well, for which a partonic interpretation is only implicit, and where the need for simpler ansätze remains.

The plan of this letter is the following. In section 2 we summarize the main features of our model for virtual-photon interactions, and in section 3 how the model can be extended to encompass an assumed longitudinal-photon contribution as well. Some comparisons, between the more sophisticated approach of having PDF's for longitudinal photons and the simpler one of x -independent multiplicative factors, are presented in section 4. Finally, some conclusions are drawn in section 5.

2 A Model for Photon Interactions

In this section we summarize the model presented in [1, 2]. It starts from the model for real photons in [9], but further develops this model and extends it also to encompass the physics of virtual photons. The physics has been implemented in the PYTHIA generator [10], so that complete events can be studied under realistic conditions.

Photon interactions are complicated since the photon wave function contains so many components, each with its own interactions. To first approximation, it may be subdivided into a direct and a resolved part. (In higher orders, the two parts can mix, so one has to provide sensible physical separations between the two.) In the former the photon acts as a pointlike particle, while in the latter it fluctuates into hadronic states. These fluctuations are of $\mathcal{O}(\alpha_{\text{em}})$, and so correspond to a small fraction of the photon wave function, but this is compensated by the bigger cross sections allowed in strong-interaction processes. For real photons therefore the resolved processes dominate the total cross section, while the pointlike ones take over for virtual photons.

The fluctuations $\gamma \rightarrow q\bar{q} (\rightarrow \gamma)$ can be characterized by the transverse momentum k_{\perp} of the quarks, or alternatively by some mass scale $m \simeq 2k_{\perp}$, with a spectrum of fluctuations $\propto dk_{\perp}^2/k_{\perp}^2$. The low- k_{\perp} part cannot be calculated perturbatively, but is instead parameterized by experimentally determined couplings to the lowest-lying vector mesons, $V = \rho^0, \omega^0, \phi^0$ and J/ψ , an ansatz called VMD for Vector Meson Dominance. Parton distributions are defined with a unit momentum sum rule within a fluctuation [11], giving rise to total hadronic cross sections, jet activity, multiple interactions and beam remnants as in hadronic interactions. In interactions with a hadron or another resolved photon, jet production occurs by typical parton-scattering processes such as $qq' \rightarrow qq'$ or $gg \rightarrow gg$.

States at larger k_{\perp} are called GVMD or Generalized VMD, and their contributions to the parton distribution of the photon are called anomalous. Given a dividing line $k_0 \simeq 0.5$ GeV to VMD states, the anomalous parton distributions are perturbatively calculable. The total cross section of a state is not, however, since this involves aspects of soft physics and eikonalization of jet rates. Therefore an ansatz is chosen where the total cross section of a state scales like k_V^2/k_{\perp}^2 , where the adjustable parameter $k_V \approx m_{\rho}/2$ for light quarks. The spectrum of GVMD states is taken to extend over a range $k_0 < k_{\perp} < k_1$, where k_1 is identified with the $p_{\perp\text{min}}(s)$ cut-off of the perturbative jet spectrum in hadronic interactions, $p_{\perp\text{min}}(s) \approx 1.5$ GeV at typical energies [10]. Above that range, the states are assumed to be sufficiently weakly interacting that no eikonalization procedure is required, so that cross sections can be calculated perturbatively without any recourse to Pomeron phenomenology. There is some arbitrariness in that choice, and some simplifications are required in order to obtain a manageable description.

A real direct photon in a γp collision can interact with the parton content of the proton: $\gamma q \rightarrow qg$ (QCD Compton) and $\gamma g \rightarrow q\bar{q}$ (Boson Gluon Fusion). The p_{\perp} in this collision is taken to exceed k_1 , in order to avoid double-counting with the interactions of the GVMD states. In $\gamma\gamma$, the equivalent situation is called single-resolved, where a direct photon interacts with the partonic component of the other, resolved photon. The $\gamma\gamma$ direct process $\gamma\gamma \rightarrow q\bar{q}$ has no correspondence in γp .

As an illustration of this scenario, the phase space of γp events is shown in Fig. 1. (A corresponding plot can be made for $\gamma\gamma$, but then requires three dimensions.) Two transverse momentum scales are introduced, namely the photon resolution scale k_{\perp} and the hard interaction scale p_{\perp} . Here k_{\perp} is a measure of the virtuality of a fluctuation of the

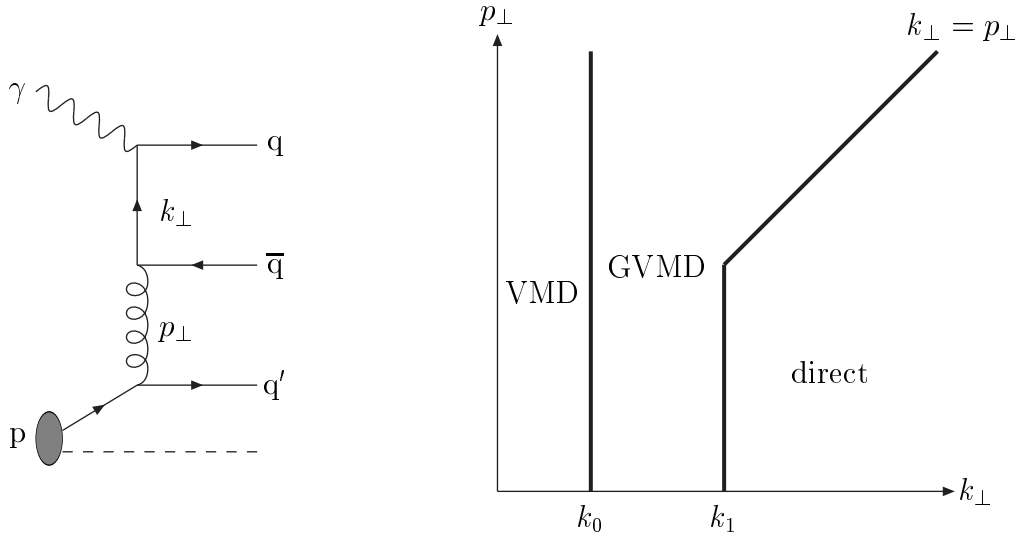


Figure 1: (a) Schematic graph for a hard γp process, illustrating the concept of two different scales. (b) The allowed phase space for this process, with one subdivision into event classes.

photon and p_\perp corresponds to the most virtual rung of the ladder, possibly apart from k_\perp . As we have discussed above, the low- k_\perp region corresponds to VMD and GVMD states that encompasses both perturbative high- p_\perp and non-perturbative low- p_\perp interactions. Above k_1 , the region is split along the line $k_\perp = p_\perp$. When $p_\perp > k_\perp$ the photon is resolved by the hard interaction, as described by the anomalous part of the photon distribution function. This is as in the GVMD sector, except that we should (probably) not worry about multiple parton-parton interactions. In the complementary region $k_\perp > p_\perp$, the p_\perp scale is just part of the traditional evolution of the proton PDF's up to the scale of k_\perp , and thus there is no need to introduce an internal structure of the photon. One could imagine the direct class of events as extending below k_1 and there being the low- p_\perp part of the GVMD class, only appearing when a hard interaction at a larger p_\perp scale would not preempt it. This possibility is implicit in the standard cross section framework.

If the photon is virtual, it has a reduced probability to fluctuate into a vector meson state, and this state has a reduced interaction probability. This can be modeled by a traditional dipole factor $(m_V^2/(m_V^2 + Q^2))^2$ for a photon of virtuality Q^2 , where $m_V \rightarrow 2k_\perp$ for a GVMD state. Putting it all together, the cross section of the GVMD sector then scales like

$$\int_{k_0^2}^{k_1^2} \frac{dk_\perp^2}{k_\perp^2} \frac{k_V^2}{k_\perp^2} \left(\frac{4k_\perp^2}{4k_\perp^2 + Q^2} \right)^2. \quad (1)$$

For a virtual photon the DIS process $\gamma^* q \rightarrow q$ is also possible, but by gauge invariance its cross section must vanish in the limit $Q^2 \rightarrow 0$. At large Q^2 , the direct processes can be considered as the $\mathcal{O}(\alpha_s)$ correction to the lowest-order DIS process, but the direct ones survive for $Q^2 \rightarrow 0$. There is no unique prescription for a proper combination at all Q^2 , but we have attempted an approach that gives the proper limits and minimizes doublecounting. For large Q^2 , the DIS $\gamma^* p$ cross section is proportional to the structure function $F_2(x, Q^2)$ with the Bjorken $x = Q^2/(Q^2 + W^2)$. Since normal parton distribution parameterizations are frozen below some Q_0 scale and therefore do not obey the gauge

invariance condition, an ad hoc factor $(Q^2/(Q^2 + m_\rho^2))^2$ is introduced for the conversion from the parameterized $F_2(x, Q^2)$ to a $\sigma_{\text{DIS}}^{\gamma^* \text{P}}$:

$$\sigma_{\text{DIS}}^{\gamma^* \text{P}} \simeq \left(\frac{Q^2}{Q^2 + m_\rho^2} \right)^2 \frac{4\pi^2 \alpha_{\text{em}}}{Q^2} F_2(x, Q^2) = \frac{4\pi^2 \alpha_{\text{em}} Q^2}{(Q^2 + m_\rho^2)^2} \sum_{\text{q}} e_{\text{q}}^2 \{xq(x, Q^2) + x\bar{q}(x, Q^2)\} . \quad (2)$$

Here m_ρ is some non-perturbative hadronic mass parameter, for simplicity identified with the ρ mass. One of the $Q^2/(Q^2 + m_\rho^2)$ factors is required already to give finite $\sigma_{\text{tot}}^{\gamma \text{P}}$ for conventional parton distributions, and could be viewed as a screening of the individual partons at small Q^2 . The second factor is chosen to give not only a finite but actually a vanishing $\sigma_{\text{DIS}}^{\gamma^* \text{P}}$ for $Q^2 \rightarrow 0$ in order to retain the pure photoproduction description there. This latter factor thus is more a matter of convenience, and other approaches could have been pursued.

In order to avoid double-counting between DIS and direct events, a requirement $p_\perp > \max(k_\perp, Q)$ is imposed on direct events. In the remaining DIS ones, denoted lowest order (LO) DIS, thus $p_\perp < Q$. This would suggest a subdivision $\sigma_{\text{LO DIS}}^{\gamma^* \text{P}} = \sigma_{\text{DIS}}^{\gamma^* \text{P}} - \sigma_{\text{direct}}^{\gamma^* \text{P}}$, with $\sigma_{\text{DIS}}^{\gamma^* \text{P}}$ given by eq. (2) and $\sigma_{\text{direct}}^{\gamma^* \text{P}}$ by the perturbative matrix elements. In the limit $Q^2 \rightarrow 0$, the DIS cross section is now constructed to vanish while the direct is not, so this would suggest $\sigma_{\text{LO DIS}}^{\gamma^* \text{P}} < 0$. However, here we expect the correct answer not to be a negative number but an exponentially suppressed one, by a Sudakov form factor. This modifies the cross section:

$$\sigma_{\text{LO DIS}}^{\gamma^* \text{P}} = \sigma_{\text{DIS}}^{\gamma^* \text{P}} - \sigma_{\text{direct}}^{\gamma^* \text{P}} \quad \longrightarrow \quad \sigma_{\text{DIS}}^{\gamma^* \text{P}} \exp \left(- \frac{\sigma_{\text{direct}}^{\gamma^* \text{P}}}{\sigma_{\text{DIS}}^{\gamma^* \text{P}}} \right) . \quad (3)$$

Since we here are in a region where the DIS cross section is no longer the dominant one, this change of the total DIS cross section is not essential.

The overall picture, from a DIS perspective, is illustrated in Fig. 2, now with three scales to be kept track of. The traditional DIS region is the strongly ordered one, $Q^2 \gg k_\perp^2 \gg p_\perp^2$, where DGLAP-style evolution [12] is responsible for the event structure. As always, ideology wants strong ordering, while the actual classification is based on ordinary ordering $Q^2 > k_\perp^2 > p_\perp^2$. The region $k_\perp^2 > \max(Q^2, p_\perp^2)$ is also DIS, but of the $\mathcal{O}(\alpha_s)$ direct kind. The region where k_\perp is the smallest scale corresponds to non-ordered emissions, that then go beyond DGLAP validity, while the region $p_\perp^2 > k_\perp^2 > Q^2$ cover the interactions of a resolved virtual photon. Comparing Figs. 1b and 2b, we conclude that the whole region $p_\perp > k_\perp$ involves no doublecounting, since we have made no attempt at a non-DGLAP DIS description but can choose to cover this region entirely by the VMD/GVMD descriptions. Actually, it is only in the corner $p_\perp < k_\perp < \min(k_\perp, Q)$ that an overlap can occur between the resolved and the DIS descriptions. Some further considerations show that usually either of the two is strongly suppressed in this region, except in the range of intermediate Q^2 and rather small W^2 . Typically, this is the region where $x \approx Q^2/(Q^2 + W^2)$ is not close to zero, and where F_2 is dominated by the valence-quark contribution. The latter behaves roughly $\propto (1-x)^n$, with an n of the order of 3 or 4. Therefore we will introduce a corresponding damping factor to the VMD/GVMD terms.

In total, we have now arrived at our ansatz for all Q^2 :

$$\sigma_{\text{tot}}^{\gamma^* \text{P}} = \sigma_{\text{DIS}}^{\gamma^* \text{P}} \exp \left(- \frac{\sigma_{\text{direct}}^{\gamma^* \text{P}}}{\sigma_{\text{DIS}}^{\gamma^* \text{P}}} \right) + \sigma_{\text{direct}}^{\gamma^* \text{P}} + \left(\frac{W^2}{Q^2 + W^2} \right)^n \left(\sigma_{\text{VMD}}^{\gamma^* \text{P}} + \sigma_{\text{GVMD}}^{\gamma^* \text{P}} \right) , \quad (4)$$

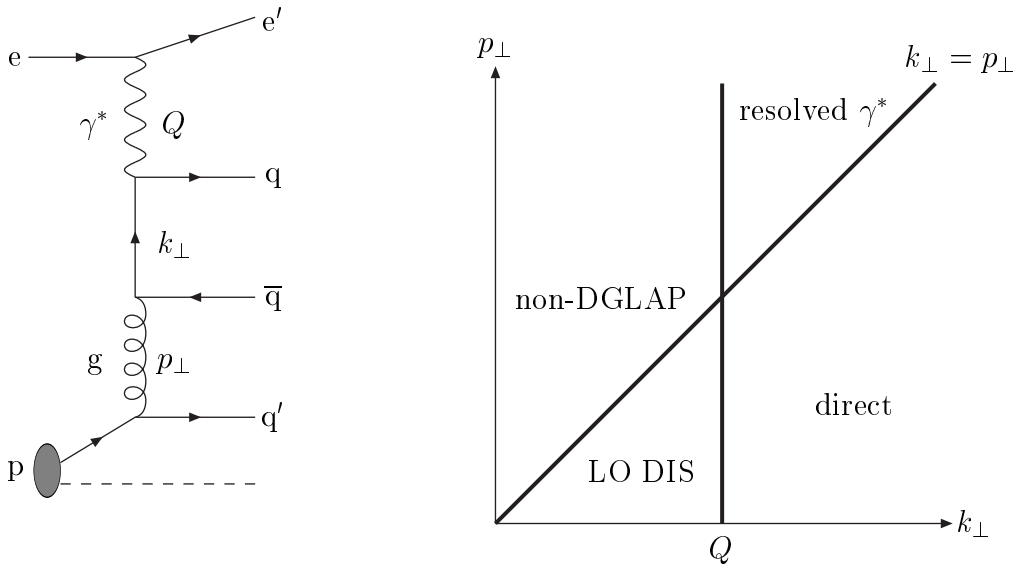


Figure 2: (a) Schematic graph for a hard γ^*p process, illustrating the concept of three different scales. (b) Event classification in the large- Q^2 limit.

with four main components. Most of these in their turn have a complicated internal structure, as we have seen. The $\gamma^*\gamma^*$ collision between two inequivalent photons contains 13 components: four when the VMD and GVMD states interact with each other (double-resolved), eight with a LO DIS or direct photon interaction on a VMD or GVMD state on either side (single-resolved, including the traditional DIS), and one where two direct photons interact by the process $\gamma^*\gamma^* \rightarrow q\bar{q}$ (direct, not to be confused with the direct process of γ^*p).

An important note is that the Q^2 dependence of the DIS and direct processes is implemented in the matrix element expressions, i.e. in processes such as $\gamma^*\gamma^* \rightarrow q\bar{q}$ or $\gamma^*q \rightarrow qg$ the photon virtuality explicitly enters. This is different from VMD/GVMD, where dipole factors are used to reduce the assumed flux of partons inside a virtual photon relative to those of a real one, but the matrix elements themselves contain no dependence on the virtuality either of the partons or of the photon itself. Typically results are obtained with the SaS 1D PDF's for the virtual (transverse) photons [11], since these are well matched to our framework, e.g. allowing a separation of the VMD and GVMD/anomalous components.

3 The Longitudinal Photon Contribution

In ep interactions, the cross section can be written as [13]:

$$\frac{d^2\sigma(ep \rightarrow e\mathbf{X})}{dy dQ^2} = f_{\gamma/e}^T(y, Q^2)\sigma_T(y, Q^2) + f_{\gamma/e}^L(y, Q^2)\sigma_L(y, Q^2) , \quad (5)$$

with the fluxes of transverse and longitudinal photons given by

$$f_{\gamma/e}^T(y, Q^2) = \frac{\alpha_{\text{em}}}{2\pi} \left(\frac{1 + (1-y)^2}{y} \frac{1}{Q^2} - \frac{2m_e^2 y}{Q^4} \right), \quad (6)$$

$$f_{\gamma/e}^L(y, Q^2) = \frac{\alpha_{\text{em}}}{2\pi} \frac{2(1-y)}{y} \frac{1}{Q^2}. \quad (7)$$

Here $y = qP/kP$ is the energy-momentum fraction carried off from the incoming electron by the virtual photon. The y or Q^2 can be traded in for the Bjorken x , but this x can be given an interpretation in terms of the momentum fraction of the struck quark in the proton only in the DIS region of large Q^2 . In e^+e^- events, an $f_{\gamma/e}^T$ or $f_{\gamma/e}^L$ occurs on each side, thus giving four terms by simple generalization of eq. (5).

The model summarized in the previous section is intended to describe in detail the σ_T term, which is composed of all the many different kinds of events. So far, nothing has been said about σ_L , except that gauge invariance dictates its vanishing in the limit $Q^2 \rightarrow 0$. However, we will assume that quite a similar decomposition can be made of longitudinal photon interactions as was done for the transverse one. To first approximation, this again means a separation into direct and resolved photons. In direct processes, the nature of the photon is explicitly included in the perturbative cross section formulae. Thus, for $\gamma^*q \rightarrow qg$ and $\gamma^*g \rightarrow q\bar{q}$, the differential cross sections $d\hat{\sigma}_T/d\hat{t}$ and $d\hat{\sigma}_L/d\hat{t}$ are separately available [14]. The latter is proportional to Q^2 and thus nicely vanishes in the limit $Q^2 \rightarrow 0$. Similarly the $\gamma^*\gamma^* \rightarrow q\bar{q}$ process gives four separate cross section formulae, $d\hat{\sigma}_{TT,TL,LT,LL}/d\hat{t}$ [6]. The DIS, non-direct part currently contains no explicit description of a longitudinal probing photon, only of a probed one. However, to the extent that PDF's are extracted from $F_2 \propto \sigma_T + \sigma_L$ data, effects may be implicitly included. Furthermore, perturbative calculations [15] predict $\sigma_L \ll \sigma_T$ in the large- Q^2 region, where this process dominates.

For resolved processes, interactions come in two kinds.

(i) Given a PDF set for the longitudinal photon, jet cross sections can be obtained by the traditional convolution of parton fluxes with the hard-scattering matrix elements. The PDF's are to be evaluated at some factorization scale μ^2 related to the hardness of the scattering, e.g. $\mu^2 = p_\perp^2 = \hat{t}\hat{u}/\hat{s}$ if Q^2 can be neglected.

(ii) In low- p_\perp interactions there is no easily definable perturbative scale μ . The relevant scale instead can be taken as the mass of the state, i.e. m_V for VMD and $2k_\perp$ for GVMD, or m_ρ if one simplifies even further, given that the ρ^0 dominates the VMD/GVMD sector (though less so at large Q^2). Such a choice is not unreasonable also from a partonic point of view: low- p_\perp means no interactions above $k_1 = p_{\perp\text{min}}(s) \approx 2m_\rho$ but certainly allows interactions below this scale, and $k_1/2$ might be a reasonable estimate of the typical order.

In the past, we have studied a few simple multiplicative expressions. Rewriting eq. (5) (for the resolved part only) as

$$\frac{d^2\sigma(\text{ep} \rightarrow \text{eX})}{dy dQ^2} = f_{\gamma/e}^T \sigma_T \left(1 + \frac{f_{\gamma/e}^L}{f_{\gamma/e}^T} \frac{\sigma_L}{\sigma_T} \right) = f_{\gamma/e}^T \sigma_T \left(1 + \frac{f_{\gamma/e}^L}{f_{\gamma/e}^T} R \right), \quad (8)$$

the forms introduced for jet production were

$$R = R_1(y, Q^2, \mu^2) = a \frac{4\mu^2 Q^2}{(\mu^2 + Q^2)^2}, \quad (9)$$

$$R = R_2(y, Q^2, \mu^2) = a \frac{4Q^2}{(\mu^2 + Q^2)}, \quad (10)$$

$$R = R_3(y, Q^2, \mu^2) = a \frac{4Q^2}{(m_\rho^2 + Q^2)}, \quad (11)$$

and for the total cross section processes

$$R = r_1(m_V^2, Q^2) = a \frac{4m_V^2 Q^2}{(m_V^2 + Q^2)^2}, \quad (12)$$

$$R = r_2(m_V^2, Q^2) = a \frac{4Q^2}{(m_V^2 + Q^2)}. \quad (13)$$

Here a in all cases denotes an unknown number, where the intention was to use $a = 1$ as an extreme contrast to the no-longitudinal-effects $a = 0$, with the truth likely to be somewhere in between. All the expressions were constructed to vanish like Q^2 for $Q^2 \rightarrow 0$. R_1 and r_1 also vanish for large Q^2 , while the rest there become Q^2 -independent. The μ -independent option R_3 essentially is the same as r_2 . In $\gamma^* \gamma^*$ events, the same approach is pursued, with one multiplicative factor for each side with a resolved photon.

It is thus this framework that should be contrasted with what is offered by a set $f_i^{\gamma^* \text{L}}(x, \mu^2)$ of PDF's for the longitudinal photon, where the dependence on parton species i and momentum fraction x_i is explicitly given. Assuming that a hard interaction at scale μ^2 is selected for the transverse photon, this entails knowledge of i and x_i . Then a sensible choice would be

$$R = R_{\text{PDF}} = \frac{Q^2}{Q^2 + m_\rho^2} \frac{f_i^{\gamma^* \text{L}}(x_i, \mu^2, Q^2)}{f_i^{\gamma^* \text{T}}(x_i, \mu^2, Q^2)}. \quad (14)$$

We have here chosen to introduce one modification for the Chýla $f_i^{\gamma^* \text{L}}$, as can be seen. His parameterizations are not intended to be valid for $Q^2 < 1 \text{ GeV}^2$ or thereabout, since the quark mass effects have not been included, which would provide a dampening in that region. In order to use them below that scale, the ad hoc multiplicative factor $Q^2/(Q^2 + m_\rho^2)$ is introduced to ensure the correct limiting behaviour for $Q^2 \rightarrow 0$, while rapidly approaching unity for $Q^2 > 1 \text{ GeV}^2$. The PDF's can then be frozen below the lowest scale for which they can meaningfully be evaluated. In the explicit calculation of $f_i^{\gamma^* \text{L}}(x_i, \mu^2, Q^2)$, the relations $0.001 \leq x_i \leq 0.995$ and $1 \leq \ln(\mu^2/\Lambda_{\text{QCD}}^2)/\ln(Q^2/\Lambda_{\text{QCD}}^2) \leq 3.9$ need to be fulfilled and are set to the relevant boundary values if not. It may lead to a negative PDF, however, wherefore the requirement $f_i^{\gamma^* \text{L}} \geq 0$ is imposed when calculating R_{PDF} .

For the studies in this article, the procedure used is to generate events based on the transverse part of resolved photons only, and then to apply one or several of the R options above as weight for the event. Thus the inclusion of resolved longitudinal-photon effects is not seen as the appearance of any new kinds of hadronic final states, but only as a more or less increased cross section for the already existing transverse-photon ones. This may not be entirely correct — any initial-state radiation would probe $f_i^{\gamma^* \text{L}}$ in the region of scales below μ^2 and momentum fractions above x_i , e.g. — but should be a good first approximation, especially in view of all the other uncertainties.

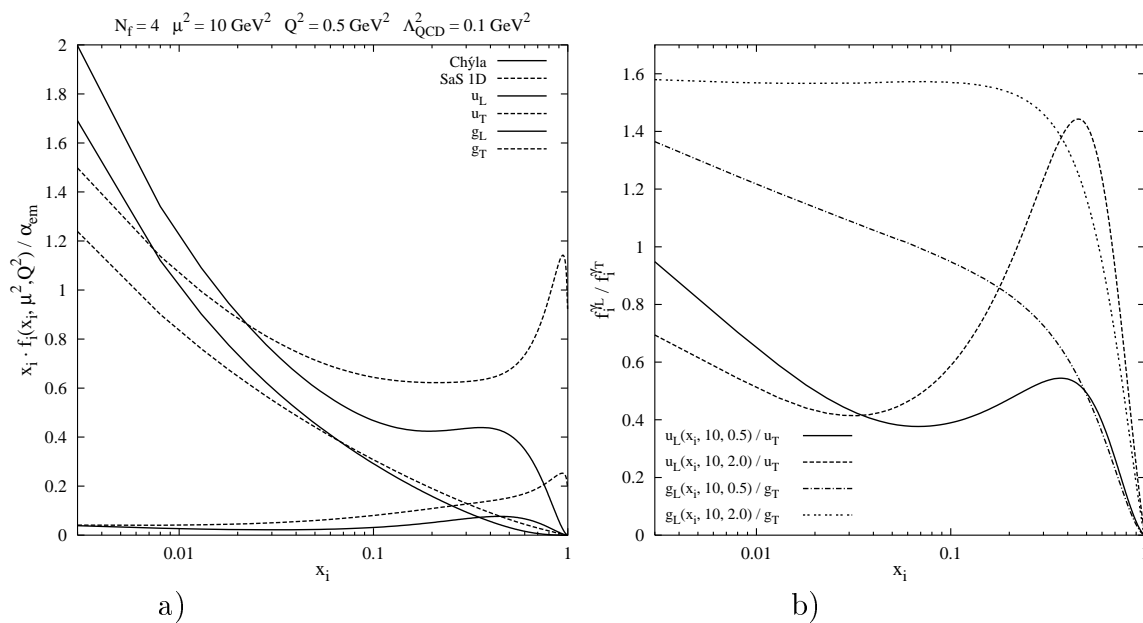


Figure 3: a) The x_i -weighted parton distribution functions as given by Chýla and SaS 1D, solid and dashed lines respectively, for a factorization scale $\mu^2 = 10 \text{ GeV}^2$ and a photon virtuality $Q^2 = 0.5 \text{ GeV}^2$. x_i is the momentum fraction carried by parton i . In falling order at small x_i the following curves are shown: the sum of the gluon and four lightest flavours (including the respective anti-flavour contribution), the gluon and the u-quark (excluding \bar{u}) contributions. b) The ratio of the Chýla and SaS 1D PDF's as a function of x_i for the u-quark and the gluon at two different photon virtualities, 0.5 and 2 GeV^2 , for a fixed factorization scale $\mu^2 = 10 \text{ GeV}^2$.

4 Some Results

The significance of the longitudinal-photon contribution depends on the $f_i^{\gamma_L^*} / f_i^{\gamma_T^*}$ ratio, but also on other factors, such as the size of the direct contribution, or the smearing of the parton-level kinematics in realistic observables. We therefore begin by a brief study of $f_i^{\gamma_L^*} / f_i^{\gamma_T^*}$ itself before illustrating experimental consequences.

The virtual photon PDF used for transversely resolved photons is the SaS 1D one [11]. In Fig. 3a it is compared to Chýla's longitudinal photon PDF as a function of the momentum fraction x_i carried by parton i . The down-type quarks give one quarter of the u-quark contribution, due to the difference in electric charge. In Chýla's PDF, no difference is made between u and c, whereas in SaS 1D charm mass effects are included, which dampens the distribution at low photon virtualities. In general, the low-end region in x_i is dominated by the gluon contribution and, with the subdivision made in SaS 1D, the major part comes from the VMD component (at this low photon virtuality). In the high- x_i end, it is instead the valence quarks that dominate and consequently the anomalous, point-like, component of the PDF. The longitudinal PDF's increase faster as compared to the transverse ones when going to lower x_i .

With $\mu^2 = 10 \text{ GeV}^2$, the u-quark and gluon ratios of the two PDF's are shown in Fig. 3b as a function of x_i for two different photon virtualities, 0.5 and 2 GeV^2 . At $x_i < 0.5$ the ratios are between 0.4 and 1.6. When increasing the photon virtuality for a fixed factorization scale μ^2 a non-trivial change in the ratios is obtained due to various effects, for example, shrinking evolution ranges and a faster dampening for the VMD

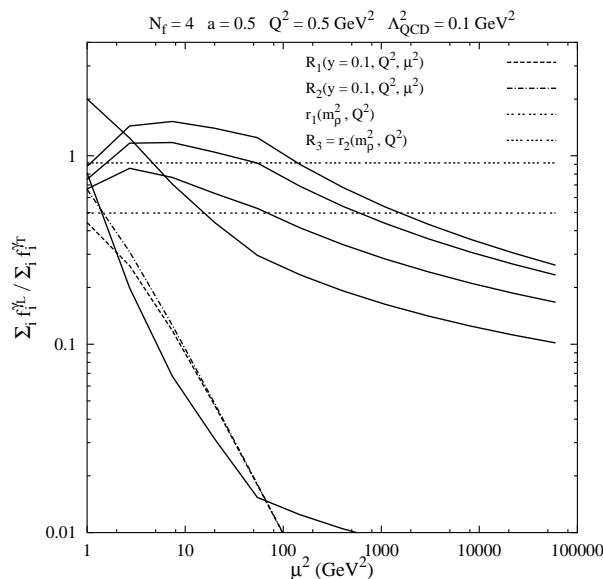


Figure 4: The ratio of longitudinal and transverse parton distributions of the photon, $\sum_i f_i^{\gamma^L} / \sum_i f_i^{\gamma^T}$, as a function of the factorization scale μ^2 for different fixed parton momentum fractions x_i . The photon virtuality is 0.5 GeV². The ratio is between the sum of the gluon and the four lightest flavours contribution for the two PDF's. In decreasing order at high μ^2 , x_i is equal to: 0.001, 0.01, 0.1, 0.5 and 0.9. $a = 0.5$ was used to calculate the different R factors.

component as compared to the anomalous one.

In Fig. 4, the PDF ratio $\sum_i f_i^{\gamma^L} / \sum_i f_i^{\gamma^T}$ is plotted as a function of the factorization scale μ^2 for different fixed x_i with a photon virtuality of 0.5 GeV². Also shown are the different R factors with $a = 0.5$. In the complete event generation, the mass of the fluctuation is used in the r_i factors (eq. (12) and (13)), i.e. m_V for VMD and $2k_\perp$ for GVMD, but for illustrative purposes the ρ^0 mass has been used for this particular distribution. Therefore, in this plot, r_2 reduces to the simple R_3 alternative. At small and medium x -values the μ^2 dependence is moderate and the μ^2 -independent r_2 alternative is a reasonable approximation to R_{PDF} . With $Q^2 = 0.5$ GeV², the r_1 alternative is about half of the r_2 one. The μ^2 -dependent factors, R_1 and R_2 , do fall off in agreement with the ratio $f_i^{\gamma^L} / f_i^{\gamma^T}$ when $x_i = 0.9$, but completely fail at smaller x_i .

We now turn to more realistic distributions, picking one γ^*p and one $\gamma^*\gamma^*$ example, where additionally the former probes jet cross sections and the latter total cross sections. The interesting range of photon virtualities, to study the longitudinal resolved photon effects, is at medium Q^2 , say in the interval $m_\rho^2 - 4$ GeV². When approaching $Q^2 = 0$ the longitudinal photon PDF vanish, and at large Q^2 the unresolved events, the direct and DIS ones in our description, take over and dominate the cross sections. In the following, the r_i factors will be used according to eq. (12) and (13), without the m_ρ approximation.

In γ^*p , a cone jet algorithm was used to find jets with transverse energy $E_\perp^{\text{jet}} > 4$ GeV within a radius $R = \sqrt{(\Delta\eta)^2 + (\Delta\phi)^2} < 1$. The invariant mass of the γ^*p system is $W_{\gamma^*p} = 200$ GeV and the photon virtuality $Q^2 = 1$ GeV². At HERA $\sqrt{s_{\text{ep}}} \simeq 300$ GeV, wherefore a fixed $y = 0.44$ was used when calculating the ratio between the longitudinal and transverse photon fluxes $f_{\gamma/e}^L(y, Q^2) / f_{\gamma/e}^T(y, Q^2)$ in eq. (8). The proton parton distribution used is the CTEQ5L [17].

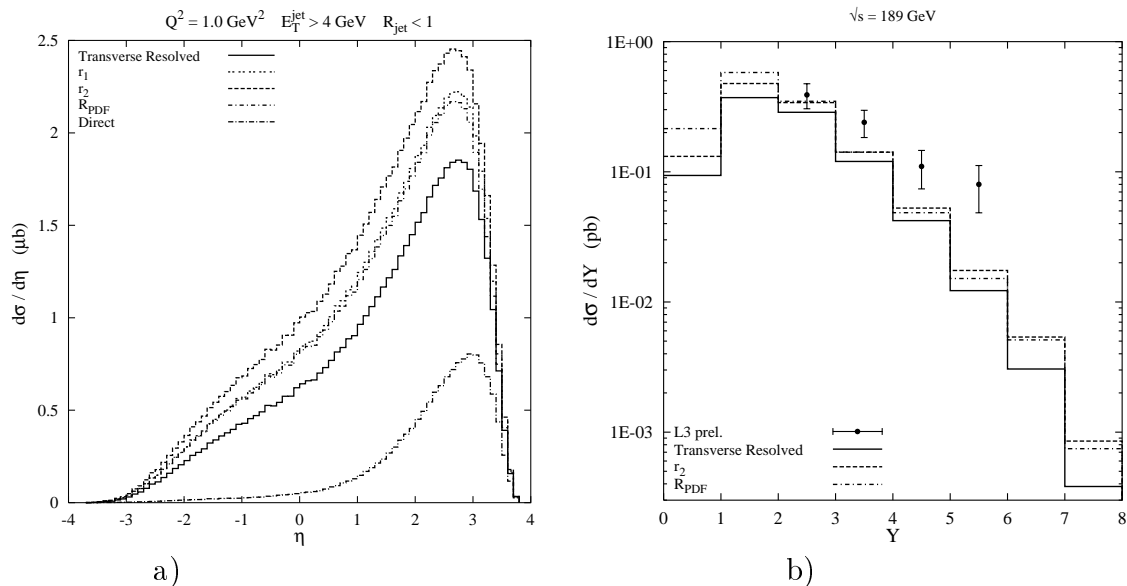


Figure 5: a) The γ^*p jet cross section as a function of the pseudo-rapidity η of the jets. ‘Direct’ shows the contribution from direct events only. The others show the total contribution of all event classes with and without R factors to include (or not include) longitudinal resolved photon effects. $a = 0.5$ is used for r_i . b) The differential $e^+e^- \rightarrow e^+e^- + \text{hadrons}$ cross section as a function of $Y = \ln(y_1 y_2 s / \sqrt{Q_1^2 Q_2^2})$. Same notation as in a).

The obtained differential jet cross section with at least one jet, with respect to the jet pseudo-rapidity η , is shown in Fig. 5a. The photon direction is along the positive y -axes. ‘Transverse Resolved’ is the total contribution from the sum of the different event classes in our model, but only taking into account the transversely resolved photon contribution. The contribution from direct events, summed over $\sigma_{\text{T,L}}$, is shown separately as a reference for the part being unaffected by the different R factors to be applied. The x_i -independent r_1 factor and the R_{PDF} factor give about the same enhancement of the jet cross section. The jet cross section with the r_2 factor is well above the other two. a was for simplicity chosen to 0.5 when calculating r_i . This was the value used in ref. [2] to obtain a nice agreement between data and the model for total γ^*p and $\gamma^*\gamma^*$ cross sections with the r_1 alternative, and also there overshoot with the r_2 one. The requirement $E_{\perp}^{\text{jet}} > 4 \text{ GeV}$, i.e. $\mu^2 \gtrsim 16 \text{ GeV}^2$, suppress the R_1 and R_2 alternatives and give only a small enhancement of the jet cross section for them.

The effects of applying the different R factors above is most pronounced at central rapidities, where the distribution is not so much contaminated by the direct events. With increasing photon virtuality, starting at small but non-negligible Q^2 , the jet cross sections obtained with r_1 and r_2 increase faster than the R_{PDF} one (all with respect to the ‘Transverse Resolved’ jet cross section). At $Q^2 = 1 \text{ GeV}^2$, as studied above, the r_1 and R_{PDF} agree, with r_2 being above. Continuing to larger virtualities, the R_{PDF} jet cross section will continue increasing relatively to the ‘Transverse Resolved’, approaching the r_2 one, with the r_1 alternative much below. At large photon virtualities the effect of the R factors will gradually decrease in importance, because the direct cross section will start to dominate the event sample. The main point, however, is that a simple x_i -independent multiplicative factor works well over the whole Q^2 range. This holds also in a simultaneous

study of two-jet event properties.

The effects of longitudinal resolved photons can be expected to be important in $\gamma^*\gamma^*$ events, if at least one of the photon virtualities is not too large. Double-tagged two photon events have been measured by the L3 collaboration [18] and is shown with respect to the variable $Y = \ln(y_1 y_2 s / \sqrt{Q_1^2 Q_2^2})$ in Fig. 5b, y_i being the energy-momentum fraction carried by photon i , Q_i^2 their respective virtuality and s the CM energy squared of the colliding e^+e^- pair.

As concluded in ref. [2], the direct contribution is the dominant part of the cross section. Again, the ‘Transverse Resolved’ is the total contribution only taking into account transversely resolved photons. The direct events are included in the total contribution with both transverse and longitudinal cross sections considered. The cross section with the r_2 alternative for estimating the longitudinal resolved photon effects, using $a = 0.5$, give about the same result as with the ratio of the longitudinal and transverse PDF’s, R_{PDF} . The result with r_1 (not shown) is between the ‘Transverse Resolved’ and r_2 . Elastic, diffractive and low- p_\perp events give a negligible contribution to this $\gamma^*\gamma^*$ cross section. With the hard scale in the processes being relatively large, small factors R_1 and R_2 are obtained. They disagree with the R_{PDF} , which is due to the rather small typical x_i values in the events (cf. Fig. 4).

At small Y , corresponding to medium x_i and large Q_i^2 , the single- and double-resolved events give small contributions, so the major part of the resolved photon events in this region comes from a photon being resolved by a DIS photon, eq. (3) (replacing direct with single-resolved). In our model, the DIS process is simply the $\gamma^*q \rightarrow q$ one and therefore only the quark part enters the R_{PDF} factor here. Typical x_i values for the lowest Y bins are ~ 0.5 , corresponding to the peak region of Fig. 3b, where $f_i^{\gamma^{\text{L}}}/f_i^{\gamma^{\text{T}}}$ is exceptionally large, and this explains why the r_2 is much below R_{PDF} here. It offers an example of a region where the x_i -dependence of $f_i^{\gamma^{\text{L}}}/f_i^{\gamma^{\text{T}}}$ cannot be ignored.

At large Y , x_i and Q_i^2 are smaller (but tagging conditions require $Q_i^2 > 3 \text{ GeV}^2$), and the single-resolved processes are most important among the resolved ones. The low x_i region is gluon-dominated and $f_i^{\gamma^{\text{L}}}/f_i^{\gamma^{\text{T}}}$ vary moderately, wherefore a simple x_i -independent factor can be well approximated for the PDF ratio. While R_{PDF} does increase with Y , already the transversely resolved photon contributions are too small to give a large effect with the R factors included, i.e. the level of the data points is not reached.

5 Summary and Outlook

The exploration of the photon structure offers challenges, both for theory and experiment. The theory challenge is to construct a realistic scenario, that covers all the aspects that we know or expect to be there. The experimental challenge is to check each of these aspects separately.

Our photon scenario involves four main components for the real photon — direct, DIS, VMD and GVMD, with the latter two corresponding to a discrete set and a continuum of resolved-photon states, respectively. For $\gamma^*\gamma^*$ interactions, the number of combinations is thirteen. Depending on photon virtualities, these are mixed in varying proportions. Each state can undergo a set of different interactions, that comprise both high- p_\perp jet production and (for most components) low- p_\perp physics. The model has several free parameters, such as parton distributions, μ^2 scales of hard processes, p_\perp cut-off scales, and non-perturbative primordial k_\perp distributions.

Needless to say, the resulting complexity makes experimental tests nontrivial. Any single distribution will receive contributions from several components, states and interactions, usually with so much overlap that it is difficult to distinguish their separate contributions. Some distributions may illuminate a special point, like the separation between direct and resolved photons in the x_γ distribution [16]. Rapidity and p_\perp distributions of jets, underlying event activity, the p_\perp distribution of the beam remnant jet, and elastic and diffractive topologies are among other measures offering a partial separation. In the future, the simultaneous study of many observables could provide further information, but probably there will be few simple answers.

In this article we have studied one further complication, namely the poorly-known structure of the resolved longitudinal photon. In principle, a separation from transverse photons is provided by the difference in y dependence between $f_{\gamma/e}^L$ and $f_{\gamma/e}^T$, but few experiments can offer the range of CM energies and tagging conditions that would allow such a separation. Since the longitudinal-photon interactions vanish in the limit $Q^2 \rightarrow 0$, the Q^2 dependence of interaction rates could offer an alternative probe. Assuming that the resolved longitudinal interactions are gradually turned on up to $Q^2 \sim m_\rho^2$, however, over that range also the interactions of the transverse photons partly change character, and furthermore direct longitudinal photons begin to contribute. It is thus not clear to what extent the structure of the longitudinal photon can be probed separately, on top of everything else.

The recent presentation of a set of QCD-evolved parton distributions for the longitudinal photon has allowed a first assessment in this letter. (Other studies, without QCD evolution, were presented in [19].) The x dependence of the Chýla PDF's clearly are different from those of the transverse photons. Therefore the ratio of the two cannot be modeled by simple x -independent factors, the way we have tried in our previous articles. It is then rather disappointing to note that most of these differences are masked in typical experimental quantities. In some instances, the resolved longitudinal-photon contribution itself is rather small relative to other event categories. Even where it is not so small, in quantities like jet rates and total $\gamma^*\gamma^*$ cross sections, the smearing in x and μ^2 is significant.

Thus it comes that a simple factor like our $r_1 = a4m_\rho^2Q^2/(m_\rho^2 + Q^2)^2$, with $a \approx 0.5$, gives quite a decent description of the resolved longitudinal effects when photon virtualities are of the order of m_ρ^2 . At larger virtualities it is dampened too fast however. (When considering total cross sections, including elastic, diffractive and low- p_\perp events, it was found to agree with data at large photon virtualities [2]. A longitudinal PDF will not give any new insight here however, since no perturbative scale can be associated with the scattering process and, moreover, other descriptions are used.) On the other hand, the $r_2 = a4Q^2/(m_\rho^2 + Q^2)$ factor was found to give a decent description of the longitudinal effects in $\gamma^*\gamma^*$ events, characterized by larger Q^2 than the jet studies, while the r_1 failed to do so. A hybrid of the two, e.g. $a4Q^2/(m_\rho^2 + bQ^2)$, could accommodate for the r_1 behaviour at $Q^2 \approx m_\rho^2$ ($b \approx 2 - 3$) and would approach a constant value for large Q^2 , similar to r_2 . With $R = a4Q^2/(m_V^2 + bQ^2)$, $a = 0.5$ and $b = 2$, approximately the same result as r_1 in the γ^*p jet cross section and as r_2 in $e^+e^- \rightarrow e^+e^- + \text{hadrons}$ ($\gamma^*\gamma^*$) are obtained (Fig. 5), i.e. in decent agreement with the parton distribution fraction R_{PDF} for both cases. It appears likely, but remains to be demonstrated, that a simple factor of this kind could work over a broad kinematical range, for various observables.

The other simple alternatives, R_1 and R_2 , are disfavoured. In particular, a significant μ^2 dependence of $f_i^{\gamma^*L}/f_i^{\gamma^*T}$ is only present at large x , and here direct processes may be

expected to dominate the data samples.

In summary, the bad news is that the experimental studies of $f_i^{\gamma_L}(x_i, \mu^2, Q^2)$ may turn out to be very difficult. The good news is that the uncertainty from a non-understanding of the resolved longitudinal photon now can be reduced, which should simplify the task of exploring other aspects of photon physics.

Acknowledgement

We thank J. Chýla for providing the parameterizations of his distributions and for helpful correspondence.

References

- [1] C. Friberg and T. Sjöstrand, *Eur. Phys. J.* **C13** (2000) 151 (hep-ph/9907245).
- [2] C. Friberg and T. Sjöstrand, LU TP 00–29 (hep-ph/0007314).
- [3] CHIO Collaboration, W.D. Shambroom et al., *Phys. Rev.* **D26** (1982) 1;
NMC Collaboration, P. Amaudruz et al., *Z. Phys.* **C54** (1992) 239;
NMC Collaboration, M. Arneodo et al., *Nucl. Phys.* **B429** (1994) 503;
E665 Collaboration, M.R. Adams et al., *Z. Phys.* **C74** (1997) 237;
ZEUS Collaboration, J. Breitweg et al., *Eur. Phys. J.* **C6** (1999) 603,
Eur. Phys. J. **C12** (2000) 393;
H1 Collaboration, C. Adloff et al., *Eur. Phys. J.* **C13** (2000) 371;
HERMES Collaboration, K. Ackerstaff et al., hep-ex/0002016.
- [4] BCDMS Collaboration, A.C. Benvenuti et al., *Phys. Lett.* **B223** (1989) 485;
H1 Collaboration, C. Adloff et al., *Phys. Lett.* **B393** (1997) 452;
HERMES Collaboration, K. Ackerstaff et al., *Phys. Lett.* **B475** (2000) 386.
- [5] J. Chýla, PRA-HEP 00-03 (hep-ph/0006232).
- [6] V.M. Budnev, I.F. Ginzburg, G.V. Meledin and V.G. Serbo,
Phys. Rept. **15** (1974) 181;
V.N. Baier, E.A. Kuraev, V.S. Fadin and V.A. Khoze,
Phys. Rept. **78** (1981) 293.
- [7] A.S. Gorski, B.L. Ioffe, A.Yu. Kodjamirian and A. Oganesian,
Z. Phys. **C44** (1989) 523.
- [8] G. Ingelman and P.E. Schlein, *Phys. Lett.* **152B** (1985) 256.
- [9] G.A. Schuler and T. Sjöstrand, *Phys. Lett.* **B300** (1993) 169,
Nucl. Phys. **B407** (1993) 539, *Z. Phys.* **C73** (1997) 677.
- [10] T. Sjöstrand, *Computer Phys. Commun.* **82** (1994) 74;
T. Sjöstrand et al., in preparation;
<http://www.thep.lu.se/~torbjorn/Pythia.html>.
- [11] G.A. Schuler and T. Sjöstrand, *Z. Phys.* **C68** (1995) 607,
Phys. Lett. **B376** (1996) 193.

- [12] V.N. Gribov and L.N. Lipatov, *Sov. J. Nucl. Phys.* **15** (1972) 438 and 675;
G. Altarelli and G. Parisi, *Nucl. Phys.* **B126** (1977) 298;
Yu.L. Dokshitzer, *Sov. Phys. JETP* **46** (1977) 641.
- [13] L.N. Hand, *Phys. Rev.* **129** (1963) 1834.
- [14] G. Altarelli and G. Martinelli, *Phys. Lett.* **76B** (1978) 89;
A. Mendéz, *Nucl. Phys.* **B145** (1978) 199;
R. Peccei and R. Rückl, *Nucl. Phys.* **B162** (1980) 125;
Ch. Rumpf, G. Kramer and J. Willrodt, *Z. Phys.* **C7** (1981) 337.
- [15] S. R. Mishra and F. Sciulli, *Phys. Lett.* **B244** (1990) 341.
- [16] ZEUS Collaboration, M. Derrick et al., *Phys. Lett.* **B322** (1994) 287;
H1 Collaboration, T. Ahmed et al., *Nucl. Phys.* **B445** (1995) 195.
- [17] CTEQ Collaboration, H. L. Lai et al., *Eur. Phys. J.* **C12** (2000) 375.
- [18] L3 Collaboration, M. Acciarri et al., *Phys. Lett.* **B453** (1999) 333.
- [19] J. Chýla and M. Tasevský, PRA-HEP 99-07 (hep-ph/9912514),
PRA-HEP 00-01 (hep-ph/0003300).